Heavy-hole and light-hole oscillations in the coherent emission from quantum wells: Evidence for exciton-exciton correlations

Arthur L. Smirl,* Martin J. Stevens, X. Chen, and O. Buccafusca
Laboratory for Photonics & Quantum Electronics, 138 IATL, University of Iowa, Iowa City, Iowa 52242
(Received 15 January 1999)

We demonstrate the presence of strong exciton-exciton correlations in GaAs-AlGaAs multiple quantum wells by using the polarization selection rules for four-wave mixing and a test that was originally designed to distinguish between quantum beats and polarization interference. We show that, when the four-wave-mixing signal is produced by two pulses that have the same circular polarization, dynamic beating behavior is observed at the heavy-hole-light-hole frequency that provides evidence of Coulomb-induced correlations that go beyond those expected from the semiconductor Bloch equations in the Hartree-Fock approximation and beyond the local field corrections used in simple phenomenological models. Moreover, this behavior cannot be explained by invoking biexcitonic effects. We demonstrate that this dynamic excitonic coupling can be explained in terms of a competition between quantum-beat-like and polarization-interference-like behavior, and we show that such behavior can be used to place quantitative limits on the coupling strength. In addition, we use a simple phenomenological model to show that excitation-induced-dephasing can produce such correlations. [S0163-1829(99)06435-8]

I. INTRODUCTION

In recent years, dephasing processes associated with nonequilibrium carriers in semiconductors and semiconductor heterostructures often have been investigated by using four-wave-mixing (FWM) techniques to monitor the decay of the coherent macroscopic polarization.[1,2] Initially, the dephasing was studied by measuring the temporally-integrated intensity or spectrum of the diffracted FWM signal.[3–7] Later, the FWM intensity was time-resolved by cross correlating it with an ultrashort laser pulse via frequency up conversion in a nonlinear crystal.[8–12] When excitons of different energies are excited, oscillations (or beats) are observed both in the time-integrated and time-resolved FWM signal. Such beats have been observed, for example, between light-hole (lh) and heavy-hole (hh) excitons[13–20] and between excitons in quantum wells of different widths.[17,21] In one such study,[17] which is of particular interest here, the behavior of the time-resolved FWM signal was used to distinguish quantum beating (which is associated with two coupled oscillators that share a common level) from polarization interference (which is associated with two independent oscillators).

Often, the beating behavior has been explained by using the single-particle density matrix equations for two independent three-level systems.[22] However, a complete description of the behavior of the FWM signal has been shown to require the inclusion of various exciton-exciton interaction phenomena,[23–27] such as local field corrections,[7,15,28–31] excitation-induced dephasing,[32–35] and biexcitons.[36–43] Various procedures have been developed for including these Coulomb-induced many-body effects in a microscopic theory. One approach is to use nonequilibrium Green's functions methods to derive the most general form of the semiconductor Bloch equations (SBE's) that include contributions of dynamical correlations and quantum kinetic processes.[44–48] Early numerical solutions have concentrated on effects such as dynamical screening within the screened Hartree-Fock approximation,[49,50] whereas the strong and ultrafast regime, in which excitonic phase space filling is the leading nonlinearity, has been investigated extensively in the unscreened Hartree-Fock approximation. More recently, the influence of dynamical correlations in the screened Hartree-Fock approximation (and modifications thereof) on the ultrafast nonlinearities has been investigated.[51] On the other hand, correlations within the $\chi^{(3)}$ regime, such as biexcitonic effects, have been found to be described within the dynamics controlled truncation scheme.[52–54]

Here, we perform time-resolved FWM measurements on a GaAs-AlGaAs multiple quantum well when the excitation spectrum is tuned so that both hh and lh excitons are excited, and we demonstrate that strong oscillations at the hh-lh beat frequency are observed when the two pump pulses have the same circular polarizations. Moreover, we use the test described in Ref. 17 to demonstrate that these oscillations behave as quantum beats, rather than polarization interference. Calculations based on the density matrix equations for two independent three-level systems indicate that polarization interference, but not quantum beats, should be observed. Similar results are expected for the SBE in the Hartree-Fock limit. Consequently, this simple test provides an elegant demonstration of the importance of including many body effects in any description of the excitonic dynamics and, more importantly, illustrates the necessity of including exciton-exciton correlations beyond the Hartree-Fock contributions. Additionally, we show that the observed quantum beating behavior can be reproduced by including a density-dependent dephasing term (so-called excitation-induced dephasing or EID). A simple phenomenological model based on EID predicts new features in the lh-hh oscillations that are quite distinct from those expected for purely quantum beating or for polarization interference. We demonstrate that these features are observed experimentally, and we use them

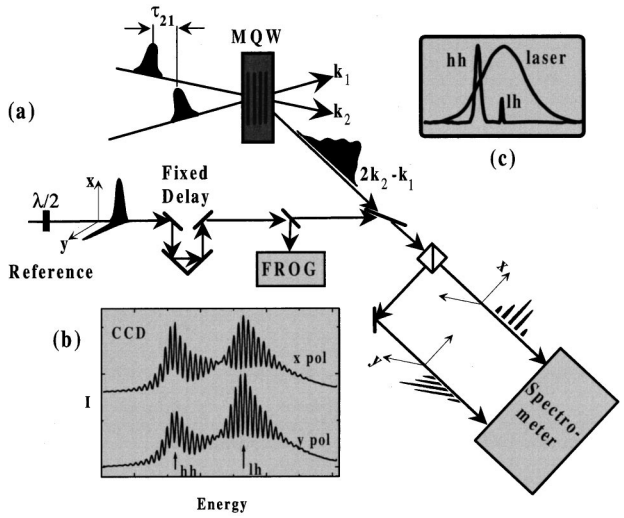

FIG. 1. (a) Spectral interferometric geometry for the dual-channel measurement of the amplitude, phase, and polarization state of the FWM signal, (b) typical spectral interferograms for the *x* and *y* components as displayed on the CCD array attached to the spectrometer, and (c) schematic showing the laser detuning with respect to the FWM power spectrum.

to place limits on the magnitude of the density-dependent dephasing.

II. DUAL-CHANNEL SPECTRAL INTERFEROMETRY

Our measurements were performed using the dual-channel spectral interferometric technique shown schematically in Fig. 1. This technique, which we have described previously,[26,27,55] allows the complete characterization of the FWM emission, including its amplitude, phase and vectorial dynamics. As shown, each pulse from our mode-locked Ti-:sapphire laser was divided into three parts. Two of the pulses [~150 fs full-width at half maximum of the intensity (FWHM)], with fields E_1 and E_2 and wave vectors $\mathbf{k}_1$ and $\mathbf{k}_2$, were used to generate the FWM signal in the direction $2\mathbf{k}_2$-$\mathbf{k}_1$ in the conventional manner. The third (reference) pulse was linearly polarized at 45°, so that it had equal *x* and *y* components. A fixed time delay was introduced between the reference pulse and the FWM signal, and the amplitude and the phase of the reference pulse were carefully measured using second-harmonic frequency-resolved optical gating (SHG-FROG).[56] The FWM signal then was allowed to interfere with the fully characterized time-delayed reference pulse by combining them collinearly. The combined signal was subsequently separated into *x* and *y* components, and each component was separately dispersed by a spectrometer. Typical spectral interferograms for the *x* and *y* components as recorded on a CCD array are shown in Fig. 1(b). They each have the form

$$I^i_{\mathrm{SI}}(\omega)=I^i_{\mathrm{FWM}}(\omega)+I^i_{\mathrm{ref}}(\omega)+2\sqrt{I^i_{\mathrm{FWM}}(\omega)}\sqrt{I^i_{\mathrm{ref}}(\omega)}\times\cos[\phi^i_{\mathrm{FWM}}(\omega)-\phi^i_{\mathrm{ref}}(\omega)-\omega\tau], \quad (1)$$

where $I^i_{\mathrm{FWM}}(\omega)$ and $I^i_{\mathrm{ref}}(\omega)$ are the spectral intensities and $\phi^i_{\mathrm{FWM}}(\omega)$ and $\phi^i_{\mathrm{ref}}(\omega)$ are the spectral phases of the FWM signal and reference pulse, respectively, and where *i* takes on the values *x* and *y* for the two polarization directions. The delay τ (typically ~5 ps) was chosen to yield fringes of a convenient spacing.

If the spectral intensity $I^i_{\mathrm{ref}}(\omega)$ and spectral phase $\phi^i_{\mathrm{ref}}(\omega)$ of each component of the reference are known, then the spectral intensity $I^i_{\mathrm{FWM}}(\omega)$ and spectral phase $\phi^i_{\mathrm{FWM}}(\omega)$ of each component of the FWM signal and the reference time delay τ can be retrieved from the corresponding spectral interferograms with a high degree of accuracy using fringe inversion techniques[57,58] that have been discussed previously. For our measurements, the spectral intensity $I^i_{\mathrm{ref}}(\omega)$ and the spectral phase $\phi^i_{\mathrm{ref}}(\omega)$ of each component of the reference pulse were independently determined from the FROG characterization. A degree of redundancy was achieved by separately measuring the spectral intensity $I^i_{\mathrm{FWM}}(\omega)$ of each component of the FWM signal by blocking the reference and measuring it with the spectrometer. Similarly, each component of the spectral intensity $I^i_{\mathrm{ref}}(\omega)$ of the reference was determined by blocking the signal and measuring it with the spectrometer. The delay τ was also confirmed using a separate calibration procedure.

The temporal amplitude $I^i_{\mathrm{FWM}}(t)$ and the temporal phase $\phi^i_{\mathrm{FWM}}(t)$ of each component were subsequently obtained by inverse Fourier transformation of the corresponding spectral amplitude and phase. In this way, the complete time-resolved vectorial dynamics, as well as the overall amplitude and phase, were measured. We emphasize that conventional time-resolved FWM techniques measure the temporal intensity, and therefore, they provide no phase information. Moreover, such techniques are scalar in nature. That is, either they monitor a single selected polarization component of the FWM signal, or they integrate over all polarization directions. In either case, conventional techniques provide little or no information about the vectorial dynamics which occur during a FWM emission process. Previously, we have shown that the vectorial dynamics contain essential information about many-body and quantum-interference effects that would be difficult to obtain using conventional techniques.[19,20,23–27]

Here, we completely time resolve the FWM emission (including the polarization dynamics) as a function of the time delay τ_{21} ($\equiv t_2-t_1$) between the two pump pulses for two input polarization configurations: (i) E_1 and E_2 having the same linear (*x*) polarization and (ii) E_1 and E_2 having the same (right) circular polarization. The measurements were performed on a sample consisting of 10 periods of ~14-nm-wide GaAs wells alternating with 17-nm-thick $Al_{0.3}Ga_{0.7}As$ barriers, which was grown on a (001)-oriented GaAs substrate. The sample was mounted onto a glass flat, the GaAs substrate was removed by selective etching to permit transmission measurements, and an antireflection coating was applied to the exposed air-semiconductor interface to reduce Fabry-Perot effects. The measurements were performed at 80 K. At this temperature, the sample had a hh linewidth of ~1.3 meV, and a hh-lh energy separation of 12 meV. The bandwidth of the excitation pulses was restricted to ~15 meV, which resulted in a measured pulsewidth of ~150 fs (FWHM). Given the hh-lh splitting, this spectral width was sufficiently broad to allow the simultaneous excitation of both lh's and hh's, yet was narrow enough to allow the ratio

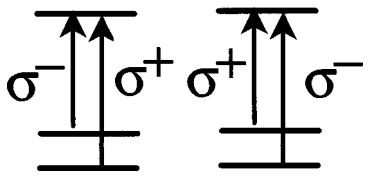

FIG. 2. Schematic of the two independent three-level (2×3) systems used to represent the hh and lh electronic transitions in the absence of many body effects, where σ^+ denotes right circularly polarized light and σ^- denotes left circular polarization.

of hh-to-lh emission to be varied over a wide range as the laser wavelength was tuned. At the fluence used here ($\sim 1\ \mu J/cm^2$), the estimated carrier density is $\sim 1.5\times 10^{16}\,cm^{-3}$ ($\sim 2\times 10^{10}\,cm^{-2}$), and the hh linewidth is further broadened to ~3.7 meV. At this operating temperature and carrier density, this sample has been separately shown to be homogeneously broadened.

III. DISTINGUISHING QUANTUM BEATS FROM POLARIZATION INTERFERENCE

As stated in the introduction, we will use a modified version of the test developed by Koch *et al.*[17] to distinguish between quantum beats and polarization interference to investigate exciton-exciton correlations. Basically, Koch *et al.*[17] recognized that the temporal FWM response of a system that consists of two nonresonant transitions that share a common level has a different dependence on the time delay τ_{21} than a system that consists of two nonresonant transitions that do not share a common level. They[17] then used this difference in the temporal behavior as a function of time delay to classify the oscillations into one of two categories: quantum beats or polarization interference. In this section, we begin by first reviewing the fundamentals of this test, then illustrate its use experimentally. Our theoretical presentation will closely parallel that of Ref. 17, but we will put the formalism into our context and notation for the reader's convenience. The results reviewed in this section then will provide a useful direct comparison for the results presented in later sections.

We will illustrate the procedure used to distinguish quantum beats from polarization interference by contrasting the FWM response of the two three-level (2×3) systems of Fig. 2 when they are excited with two pump pulses having the same linear polarization with the response of the same systems when they are excited with two pump pulses having the same circular polarization. In the simplest picture (and in the absence of many body effects), the 2×3 system and the selection rules shown in Fig. 2 can be used to represent the electronic states associated with the hh and lh transitions for the two spin states in a quantum well.

We initially assume that each pulse is linearly (x) polarized. In addition, in order to obtain the simplest description of our experiments and in order to obtain a closed form solution, we assume that the pulses in the $\mathbf{k}_2$ and $\mathbf{k}_1$ directions have delta function time dependencies given by $\delta(t)$ and $\delta(t+\tau_{21})$, respectively. Under these excitation conditions, both lh and hh transitions that share a common level in each of the 2×3 systems shown in Fig. 2 will be excited (since x-polarized light is composed of equal parts left- and right-circular polarizations). In this case, one can readily solve the density matrix equations for the two three-level systems shown in Fig. 2 to third-order. The polarization that propagates in the $2\mathbf{k}_2$-$\mathbf{k}_1$ direction is found to be proportional to

$$\mathcal{P}_{QB}\propto\Theta(t)\Theta(\tau_{21})\mathcal{E}_2^2\mathcal{E}_1^*\exp[-\gamma(t+\tau_{21})]\times\{[1+A\exp(i\Omega\tau_{21})][1+A\exp(-i\Omega t)]\}\hat{\mathbf{x}},\quad(2)$$

where Θ denotes the Heaviside step function, $\mathcal{E}_1$ and $\mathcal{E}_2$ are the slowly varying electric field amplitudes of the two pump pulses, γ is the dephasing rate, $\hbar\Omega$ is the difference between the hh and lh energies, and A is a phenomenological constant that reflects the relative strength of the lh FWM emission. In our case, A is the product of the square of the ratio of the lh and hh optical transition matrix elements ($\sim\frac{1}{3}$) and a spectral weighting factor (~2) to account for the detuning of the excitation wavelength with respect to the hh and lh excitons, as shown schematically in Fig. 1(c). Furthermore, we have assumed that the dephasing is much faster than the population decay.

The slowly varying polarization amplitude given by Eq. (2) is written from the frame of reference of the hh exciton. Thus, the term $[1+A\exp(-i\Omega t)]$ in Eq. (2) is the sum of two oscillators: The first represents the polarization oscillating at the hh frequency, and the second at the lh frequency. However, these oscillators are not independent. The initial (at $t=0$) relative phases and amplitudes of the two oscillators are fixed at a value determined by the factor $[1+A\exp(i\Omega\tau_{21})]$ which multiplies both oscillators. This coupling is a consequence of the shared level, and in this sense, the ''interference'' or beating takes place within the material. The magnitude of the total polarization (and therefore of the net emitted field) oscillates at the beat frequency Ω with a phase that is independent of τ_{21}.

The signal generated in the detector is proportional to the intensity and, therefore, it is proportional to

$$S_0\propto|\mathcal{P}_{QB}|^2\propto\Theta(t)\Theta(\tau_{21})I_2^2I_1\exp[-2\gamma(t-\tau_{21})]\times\{1+2A^2+A^4+2(A+A^3)\cos\Omega\tau_{21}+2(A+A^3+2A^2\cos\Omega\tau_{21})\cos\Omega t\}.\quad(3)$$

Notice that the only term that oscillates in time is the last one, which is proportional to $\cos\Omega t$. Consequently, it is evident that the peaks of this oscillation occur at times t_p given by

$$t_p=m(2\pi/\Omega),\quad(4)$$

where m is an integer which labels successive peaks. Thus, the position of a given peak does not depend on τ_{21}. The slope of the t_p versus τ_{21} curve is 0. Such oscillations were classified in Ref. 17 as quantum beats.

By contrast, if the two independent three-level systems shown in Fig. 2 are excited with two right-circularly polarized pulses, only the lh transition on the left and the hh transition on the right will be excited. In this case, the two excited oscillators share no common level, and the FWM polarization that propagates in the $2\mathbf{k}_2$-$\mathbf{k}_1$ direction is proportional to

$$\mathcal{P}_{\mathrm{PI}} \propto \Theta(t)\Theta(\tau_{21})\mathcal{E}_2^2\mathcal{E}_1^* \exp[-\gamma(t+\tau_{21})] \times\{1+A^2\exp[-i\Omega(t-\tau_{21})]\}\hat{\sigma}_+, \quad (5)$$

where $\hat{\sigma}_+$ denotes right circularly polarized light. The slowly varying polarization amplitude given by Eq. (5) again is written from the frame of reference of the ''hh'' exciton. In this case, Eq. (5) is the sum of two independent oscillators: The first represents the polarization oscillating at the hh frequency, and the second the polarization oscillating at the lh frequency with an independent phase determined by τ_{21}. The magnitude of the total polarization (and therefore of the net emitted field) oscillates at the beat frequency Ω with the phase determined by τ_{21}, but there is no interaction (or interference) between the two polarizations within the material. Each propagates and oscillates independently. In this sense, the beating does not originate within the material.

Again, the signal generated in the detector is proportional to the intensity and is proportional to

$$S_0 \propto |\mathcal{P}_{\mathrm{PI}}|^2 \propto \Theta(t)\Theta(\tau_{21})I_2^2 I_1 \exp[-2\gamma(t+\tau_{21})] \times\{1+A^4+2A^2\cos[\Omega(t-\tau_{21})]\}. \quad (6)$$

In this case, we see that the oscillations are a consequence of the nature of the detection process. Such oscillations were classified as polarization interference in Ref. 17. It is also evident from this expression that the peak of each oscillation occurs at a time given by

$$t_p = \tau_{21} + m\left(\frac{2\pi}{\Omega}\right). \quad (7)$$

Thus, one would expect to observe a linear relationship between each peak and the time delay τ_{21} for polarization interference.

Based on a similar analysis, Koch *et al.*[17] suggested that one could distinguish quantum beats from polarization interference by simply plotting the position of each peak t_p in the time-resolved FWM signal as a function of the time delay τ_{21}. The result should be a straight line. The slope of the line will be zero if the time-resolved oscillations are the result of quantum beating, and the slope will be unity if they originate from polarization interference. (Note that we have taken our origin to coincide with the $\mathcal{E}_2$ pulse. If the origin is taken to coincide with the $\mathcal{E}_1$ pulse, as was done in the original paper,[17] then a slope of 1 will be obtained for quantum beating and a slope of 2 for polarization interference.) We emphasize that many body effects are not included in the analysis to this point.

To illustrate this procedure and to test whether the hh-lh oscillations in our previous publication[20] were the result of quantum beats or polarization interference, we performed this test on the FWM emission from our sample. Specifically, the laser wavelength was tuned onto the lh exciton so that both hh's and lh's were strongly excited. We used the geometry shown in Fig. 1 to completely time resolve the FWM emission (including the polarization dynamics) as a function of time delay τ_{21} between the pump pulses. Measurements were performed, first, for E_1 and E_2 having the same linear (x) polarization state and, then, for E_1 and E_2 having the same (right) circular polarization state.

In Fig. 3(a), we show the total intensity S_0 of the time-resolved FWM signal for various time delays τ_{21} between the pump and probe pulses when the sample was excited with two x-polarized pump pulses. The ellipticity angle and the orientation of the polarization ellipse were also time resolved. To within our experimental accuracy, the FWM signal was found to be linearly and x polarized for all times and all time delays. For this reason, we plot only the total intensity in Fig. 3(a). Clearly, oscillations at the hh-lh beat frequency are observed at each delay shown. In Fig. 3(b), we plot the position of each peak t_p in the time-resolved FWM signal [indicated by the arrows in Fig. 3(a)] as function of the time delay τ_{21}, for a more complete set of time delays. Clearly, the slope is zero for each peak. Consequently, the oscillations shown in Fig. 3 behave as quantum beats and not polarization interference. This is exactly the behavior that we would have expected from a simple density matrix model for the 2×3 system shown in Fig. 2 (without many-body effects) based on Eq. (3).

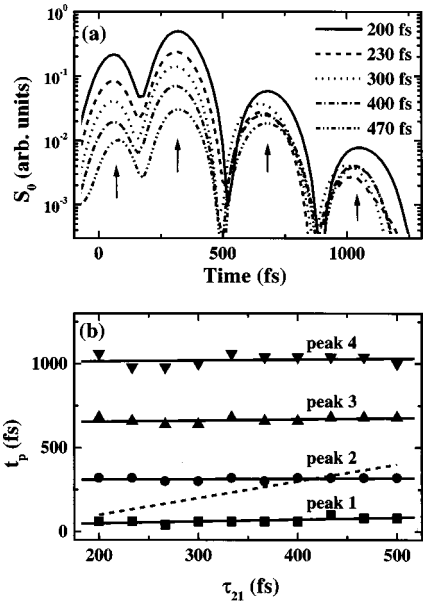

FIG. 3. Results of measurements to distinguish quantum beating from polarization interference using two linearly x-polarized incident pump pulses: (a) Time-resolved measurements of the total intensity S_0 of the FWM intensity for selected time delays τ_{21} between two incident pulses, and (b) the time t_p at which each peak [indicated by an arrow in (a)] occurs as a function of τ_{21}, for a more complete set of time delays. The dotted line indicates a slope of unity.

IV. A TEST FOR EXCITON-EXCITON CORRELATIONS

The results of performing the test to distinguish quantum beats from polarization interference when the sample is excited with two pulses that have the same (right) circular polarization are shown in Fig. 4. In Fig. 4(a), the results of measuring the time-resolved FWM signal for selected time delays τ_{21} between the pump and probe pulses are shown. Again, the polarization state was also measured, and the FWM signal was found to be right circularly polarized for all times and all time delays. As for the linear excitation pulses [i.e., Fig. 3(a)], pronounced oscillations at lh-hh beat frequency are evident. In Fig. 4(b), the position of each peak in

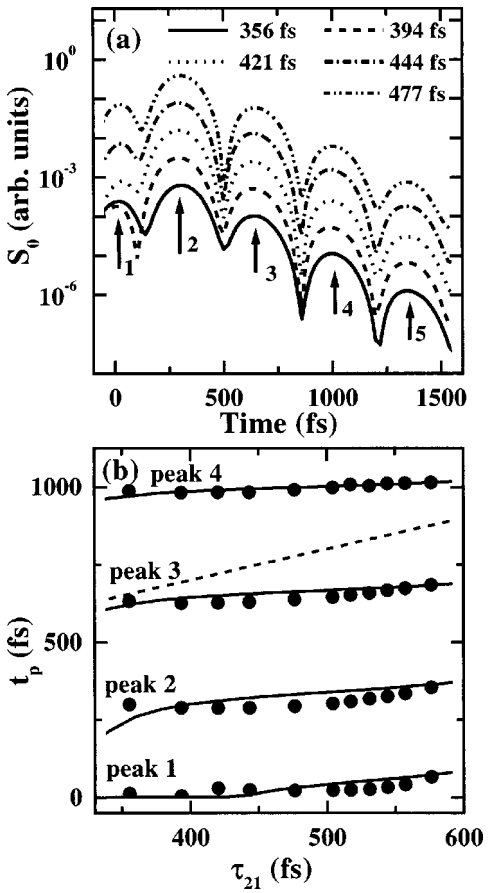

FIG. 4. Results of measurements to distinguish quantum beating from polarization interference using two right-circularly polarized pump pulses: (a) Time-resolved measurements of the total intensity S_0 of the FWM intensity for selected time delays τ_{21} between the two incident pulses in the range between 350 and 600 fs, and (b) the time t_p at which each peak [indicated by the first four arrows in (a)] occurs as a function of τ_{21}, for a more complete set of time delays. The dotted line indicates a slope of unity, and the solid lines are the result of simulations based on Eq. (9).

the time-resolved FWM signal [indicated by the arrows in Fig. 4(a)] is plotted as function of the time delay τ_{21}, again for a more complete set of delays. The slope of each curve is approximately zero, not unity. Consequently, the oscillations produced when the sample is excited by two right circularly polarized pulses satisfy the criterion for quantum beats, not polarization interference. Since quantum beats would not be expected for two independent three-level systems without many body effects [see Eq. (5)], this result suggests that the two excitonic systems are not independent, but are coupled and correlated. It should also be noted that the SBE, in their original form (i.e., in the Hartree-Fock limit, without EID or biexciton formation included), would also be expected to predict polarization interference, but no quantum beating, when two right circularly polarized pulses are used. Consequently, the observation of quantum-beat-like behavior suggests a correlation beyond the Hartree-Fock contribution. These measurements are consistent with other[19,20,54] recent observations.

V. COUPLING BY EXCITATION-INDUCED-DEPHASING

The quantum-beating-like behavior shown in Fig. 4 requires the inclusion of a process that strongly couples the two spin systems shown in Fig. 2. One such process, which has been invoked previously,[32] is EID. EID can be included in the SBE,[33] but analytical solutions to the full SBE are not possible, and in general, the SBE require lengthy numerical solution. The simplest approach is to solve the density matrix equations for the two three-level systems shown in Fig. 2 and to include EID phenomenolgically by expanding the dephasing rate in a Taylor series and keeping the first two terms:

$$\gamma(n)=\gamma_0+\frac{\partial\gamma}{\partial n}n=\gamma_0+N\frac{\partial\gamma}{\partial n}(\rho_{ee}^{+}+\rho_{ee}^{-}), \tag{8}$$

where γ_0 is the low density dephasing rate at the operating lattice temperature and $n=N(\rho_{ee}^{+}+\rho_{ee}^{-})$ is the total density of excited excitons, regardless of spin. Here, N denotes the total density of oscillators of each spin system and $\rho_{ee}^{+}(\rho_{ee}^{-})$ denotes the upper level population matrix element for the spin $-\frac{1}{2}$ $(+\frac{1}{2})$ system. Because it is the total population that determines the dephasing rate, this term provides a coupling between the two three-level systems.

One can readily obtain a closed form solution to these modified density matrix equations for right circular excitation pulses by making the same approximations that we have made throughout (namely, by assuming delta function time dependences for the excitation pulses and by assuming that the dephasing is much faster than the population decay). Under these circumstances, the FWM polarization that propagates in the $2\mathbf{k}_2$-$\mathbf{k}_1$ direction is found to be proportional to

$$\mathcal{P}_{\mathrm{EID}}\propto\Theta(t)\Theta(\tau_{21})\mathcal{E}_2^2\mathcal{E}_1^{*}\exp[-\gamma(t+\tau_{21})]\times\left\{[1+A^2\exp(-i\Omega(t-\tau_{21}))]+\left(\frac{\eta t}{2\hbar}\right)\times[(1+A\exp(i\Omega\tau_{21}))(1+A\exp(-i\Omega t))]\right\}\hat{\sigma}^{+}, \tag{9}$$

where the parameter $\eta\equiv 2N\hbar(\partial\gamma/\partial n)$, which has units of energy, is the EID parameter that we have used in previous publications,[23–27] and it is a measure of the strength of the density dependence of the dephasing. Equation (9) basically consists of two terms (each enclosed in square brackets). The first term (in square brackets) has the same form as the FWM polarization that we have associated with polarization interference [see Eq. (5)], and the second term, which is multiplied by $\eta t/2\hbar$, has the same form as the FWM polarization that we have associated with quantum beats [see Eq. (2)].

There are two limits of immediate interest: $\eta t/2\hbar\ll 1$ and $\eta t/2\hbar\gg 1$. When $\eta t/2\hbar\ll 1$ for all times of interest, Eq. (9) reduces to the result that would be obtained for the two independent, uncoupled three-level systems shown in Fig. 2 [i.e., to Eq. (5)]. As we have already stated, in this case, the lh transition is excited in the system on the left, and the hh transition is excited in the system on the right. Under these conditions, the optically excited transitions share no common level, and there is no coupling between the excited states in the two independent systems. The latter conditions clearly correspond to polarization interference. In this limit, the detected intensity is given by Eq. (6) for polarization interference, and thus, there is a linear relationship between the peak

of one of the oscillations in time t_p and the time delay τ_{21}, as predicted by Eq. (7). This limit ($\eta=0$) is represented by the dotted line in Fig. 4(b).

By comparison, if $\eta t/2\hbar \gg 1$, the light is still directly coupled only to the lh transition on the left and the hh transition on the right in Fig. 2. That is, the optically-excited transitions still technically share no common level, but now the upper levels are strongly coupled through the density-dependent dephasing given by Eq. (8). In this limit, using Eq. (9), we find the total FWM intensity to be proportional to

$$S_0 \propto |\mathcal{P}_{\mathrm{EID}}|^2 \propto \Theta(t)\Theta(\tau_{21}) I_2^2 I_1 (\eta t/2\hbar)^2 \exp[-2\gamma(t+\tau_{21})]\{1 + 2A^2 + A^4 + 2(A+A^3)\cos\Omega\tau_{21} + 2(A+A^3+2A^2\cos\Omega\tau_{21})\cos\Omega t\}. \quad (10)$$

Except for the multiplicative factor of $(\eta t/2\hbar)^2$, Eq. (10) is mathematically equivalent to Eq. (3). Thus, we see that in the strong coupling limit the effects of EID are mathematically equivalent to sharing a common level, even though there is clearly a physical difference. In this limit, as with Eq. (3), the slope of the t_p versus τ_{21} curve is 0, which is identical to the slope exhibited by the data shown in Fig. 4. This is the type of behavior that previously has been attributed to quantum beating.

The solid curves in Fig. 4(b) are the results of simulations using the full FWM polarization given by Eq. (9) with $\eta = 4$ meV and $\Omega = 2\pi/340\ \mathrm{fs}^{-1}$, and they demonstrate that this model produces qualitative and quantitative agreement with the data presented to this point. However, Eq. (9) predicts new features in the hh-lh oscillations that are not characteristic either of pure quantum beating or of polarization interference. For example, as we explained earlier, the first term in square brackets in Eq. (9) produces a response that is characteristic of polarization interference and the second term in square brackets (which is multiplied by $\eta t/2\hbar$) produces a response that resembles quantum beating. Since the second term is proportional to time, it will be negligible for times $t \ll 2\hbar/\eta$ and dominant for $t \gg 2\hbar/\eta$. In other words, for the parameters given here, Eq. (9) predicts a transition from polarization-interference-like behavior to quantum-beating-like behavior on a characteristic time scale of $2\hbar/\eta \sim 330$ fs (for $\eta = 4$ meV). It is very difficult to unambiguously distinguish a transition of this duration occurring near $t=0$ because of the finite width of our pulses (which are not currently taken into account in our model).

Equation (9) also predicts a dynamic, periodic competition between the two types of oscillations as a function of time delay τ_{21}, with a period equal to the lh-hh beat frequency. Inspection of Eq. (9) reveals that the ''quantum-beating'' term is not only multiplied by $\eta t/2\hbar$, but is proportional to $[1+A\exp(i\Omega\tau_{21})]$. Consequently, the contribution of the term that we have associated with ''quantum beating'' will be periodically reduced with respect to the term that we have associated with ''polarization interference''. A minimum in the ''quantum beating'' term will occur each time τ_{21} is an odd multiple of π/Ω. The consequences of this behavior are illustrated in Fig. 5, where the simulated time-resolved FWM signals [calculated using Eq. (9)] are shown for equally spaced time delays between 300 and 667 fs. Notice that for time delays τ_{21} near 510 fs ($\sim 3\pi/\Omega$) the positions of the peaks in the FWM signal are shifted, the oscillations are distorted, and their amplitudes are dramatically reduced at early times t. At longer times t (as $\eta t/2\hbar$ becomes larger and the ''quantum beating'' term increases in strength), the oscillations become stronger, their periods more regular, and the positions of the beat maxima more quantum-beat-like. Similar behavior is consistently observed in the data, as illustrated in Fig. 6.

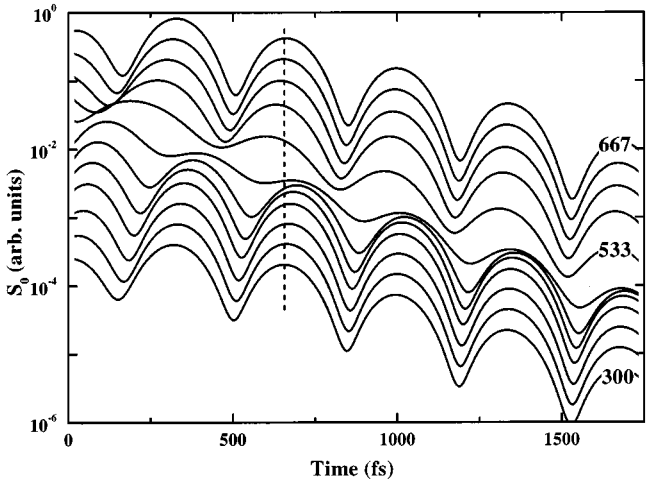

FIG. 5. Calculations of the total intensity S_0 of the FWM intensity as a function of time for equally spaced time delays τ_{21} between the two incident pulses in the range between 300 and 667 fs.

Careful comparison of Figs. 5 and 6 shows that the minimum in the ''quantum beating'' contribution in the data occurs at a time delay that is shifted by $\sim$140 fs compared to the minimum in the simulations. We do not know the origin of this shift, and it is the subject of ongoing investigation; however, we speculate that it is a consequence of our assuming delta function excitation pulses. The actual excitation pulses are each $\sim$150 fs in duration, and the frequencies which are resonant with the hh exciton have been determined to have phases that are slightly different from those that are resonant with the lh. Consequently, with the exception of the

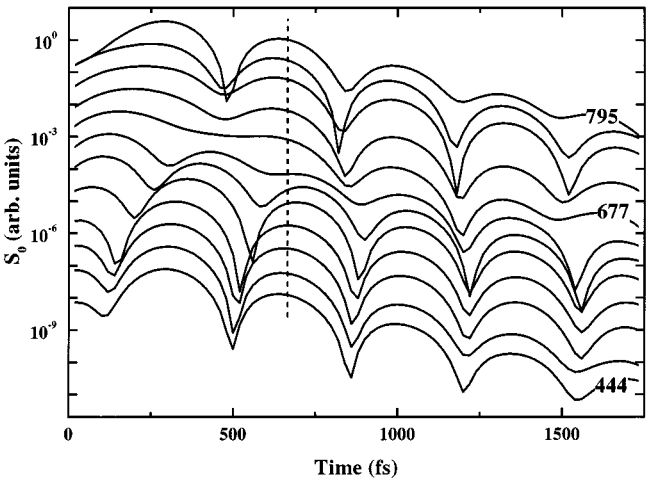

FIG. 6. Measurements of the total intensity S_0 of the FWM intensity as a function of time for equally spaced time delays τ_{21} between the two incident pulses in the range between 444 and 795 fs.

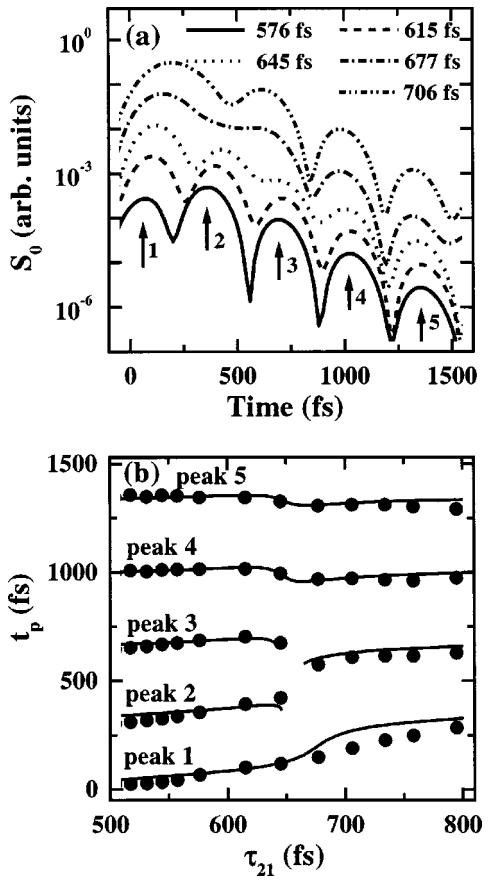

FIG. 7. (a) Time-resolved measurements of the total intensity S_0 of the FWM intensity for selected time delays τ_{21} between the two incident pulses in the range between 500 and 800 fs and (b) the time t_p at which each peak [indicated by the arrows in (a)] occurs as a function of τ_{21}, for a more complete set of time delays. The solid lines are the result of simulations based on Eq. (9).

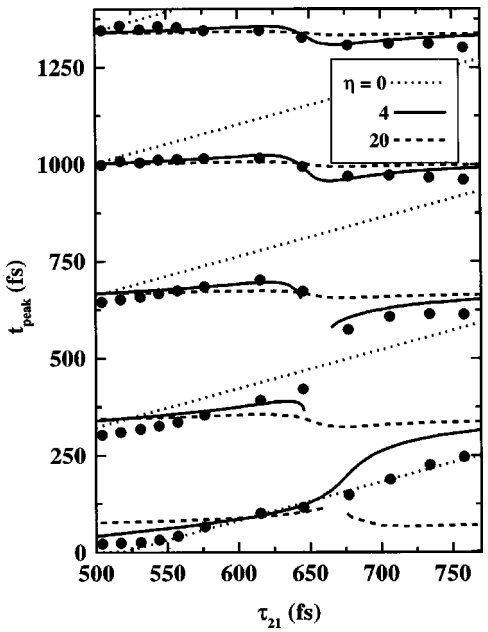

FIG. 8. Comparison between the measured (solid dots) and the simulated time t_p at which each peak in the lh-hh oscillations occurs as a function of τ_{21} for three values of the EID parameter: $\eta=0$ (dotted line), 4 (solid line), and 20 meV (dashed line).

simulations shown in Fig. 5, the time delays for all simulations have been shifted by 140 fs to facilitate a direct comparison with the data.

The new features described above, which are not characteristic of quantum beating or polarization interference, and the excellent agreement between the data and the simulations based on Eq. (9) are also apparent if both data and simulation are plotted in the conventional format used to discriminate quantum beats from polarization interference (e.g., see Figs. 3 or 4). Figure 7 shows a plot of the temporal position of the peak in the lh-hh oscillations as a function of delay between the two pump pulses. This figure differs from Fig. 4 in that it focuses on the behavior at longer time delays in the vicinity of a minimum in the quantum beating term. Clearly, the data in this region can not be described by a straight line with slope of either 0 or 1 as required by quantum beating or polarization interference, respectively, acting individually. Simulations based on Eq. (10) (i.e., the solid lines in Fig. 7) do, however, produce good agreement with the data.

VI. ESTIMATE OF THE COUPLING STRENGTH

We emphasize that this technique isolates, and is particularly sensitive to, the strength of the Coulomb-induced correlations, or coupling, between the excitons. We now illustrate that sensitivity by using the simple model that we have described in our previous work.[24,25] That model[24] phenomenologically includes EID, local field effects and biexciton formation. The local-field effects will not provide a resonant coupling between the two spin systems, and therefore, they can be neglected. Moreover, the technique described here prevents the formation of pure biexcitons involving either two hh excitons or two lh excitons of opposite spin by using two excitation pulses with the same circular polarizations. However, under these excitation conditions, mixed biexcitons can be formed from one hh exciton and one lh exciton having opposite spins. Mixed hh-lh biexcitons have been observed in ZnSe quantum wells, but their contribution to the FWM signal was found to be roughly an order of magnitude weaker than that of hh biexcitons.[59] We have examined our FWM spectra for evidence of mixed lh-hh biexciton formation when we excite with two right circularly polarized pulses, and we find no resolvable signal at the expected mixed biexciton frequency (to within our experimental accuracy under our excitation conditions). For these reasons, we neglect the contributions of mixed lh-hh biexcitons here. Consequently, within the context of this phenomenological model, only EID can provide the needed coupling. Therefore, when the sample is excited with two pulses having the same circular polarization, the model that we have used previously reduces to the one used in the previous section. Moreover, the features displayed in Figs. 4–7 allow a rough quantitative estimate of the strength of the EID coupling between the two spin systems, again, within the context of the model presented here.

Figure 8 illustrates the sensitivity of this technique to the EID parameter. This figure shows a comparison between the data and simulations using three values of the EID parameter: $\eta=0$, 4, and 20 meV. Notice that $\eta=0$ produces reasonable agreement at early times t, when EID effects are

expected to be negligible (i.e., $t \ll 2\hbar/\eta$), for all time delays τ_{21}, but this value produces poor agreement at later times (when $t > 2\hbar/\eta$). By comparison, $\eta = 20$ produces acceptable agreement with the data at later times when EID effects are expected to dominate, but poor agreement for earlier times. Of the three values shown here, only $\eta = 4$ produces acceptable agreement at all times. The simulated solid curves shown in Figs. 4, 5, and 7 were all produced using this value for the EID parameter. From a comparison with the data presented in this work only, we estimate the EID parameter to be 4 ± 2 meV.

Our principal point is not that EID is the only process that can produce the quantum-beating-like behavior shown in Figs. 4–8 (although we have shown this interpretation to be consistent with the simple phenomenological model which has been successful in accounting many other features in our FWM data[24,25]). A rigorous analysis should be based on a detailed microscopic theory. Once such a calculation is performed, the procedure described here can be used to evaluate the strength of the exciton-exciton correlations in that model in the same way that we have used it here to evaluate the EID parameter.

VII. CONCLUSION

The data and calculations presented here demonstrate that, when excitation pulses with the same circular polarizations are used, the test that was originally designed to distinguish quantum beats from polarization interference becomes an effective test for Coulomb-induced excitonic correlations that go beyond the Hartree-Fock contributions (or, in terms of the phenomenological model used in this paper, beyond the local field effects).[60] Moreover, these correlations are in addition to biexcitonic effects, since biexcitonic contributions are found to be negligible when a single circular polarization is used for both pump pulses. In fact, the data presented in Figs. 4–8 suggest that these correlations are not only important, but that they dominate the FWM response under these excitation conditions. Finally, the features observed here make it clear that the coupling between the spin systems is dynamic, rather than static. While hh-lh mixing of the valence band states (e.g., as the result of strain or quantum confinement) can conceptually provide a coupling between the two spin systems, such a mixing would produce a static coupling, and therefore, it can not explain the dynamic results discussed here.

A secondary point to be made concerning the results presented here is that the classification of lh-hh oscillations as quantum beats or polarization interference is problematic and, perhaps, overly simplistic. If one accepts the definition that oscillations arising from interference within the sample are quantum beats (and, conversely, that oscillations arising from interference at the detector are polarization interference) then, in this sense, the oscillations arising from the exciton-exciton correlations (Fig. 7) and those arising from a shared common level (Fig. 3) are both quantum beats. However, the beats arising from the exciton-exciton correlations are clearly fundamentally different from the beats arising from lh and hh transitions that share a common level. The coupling is dynamic in the case of the former, and the sharing is a static condition for the latter. Finally, it can be argued that the term ''quantum beats'' should be reserved for measuring oscillations that directly monitor the Raman coherence terms. In the latter sense, all of the phenomena that we have discussed here must be classified as polarization interference, since two-pulse self-diffraction FWM geometries do not monitor the Raman coherence directly (see Refs. 61 and 62 for a discussion of this latter point).

ACKNOWLEDGMENTS

The authors gratefully acknowledge numerous insightful conversations with Rolf Binder. This research was supported in part by the National Science Foundation and the U.S. Army Research Office.

*FAX: (319) 335-3462. Electronic address: art-smirl@uiowa.edu

[1] *Coherent Optical Interactions in Semiconductors*, edited by R. T. Phillips (Plenum, New York, 1994), and references therein.
[2] J. Shah, *Ultrafast Spectroscopy of Semiconductors and Nanostructures* (Springer-Verlag, Heidelberg, 1996), and references therein.
[3] L. Schultheis, M. D. Sturge, and J. Hegarty, Appl. Phys. Lett. **47**, 995 (1985).
[4] L. Schultheis, A. Honold, J. Kuhl, K. Köhler, and C. W. Tu, Phys. Rev. B **34**, 9027 (1986).
[5] L. Schultheis, J. Kuhl, A. Honold, and C. W. Tu, Phys. Rev. Lett. **57**, 1635 (1986).
[6] L. Schultheis, J. Kuhl, A. Honold, and C. W. Tu, Phys. Rev. Lett. **57**, 1797 (1986).
[7] K. Leo, M. Wegener, J. Shah, D. S. Chemla, E. O. Göbel, T. C. Damen, S. Schmitt-Rink, and W. Schäfer, Phys. Rev. Lett. **65**, 1340 (1990).
[8] S. T. Cundiff and D. G. Steel, IEEE J. Quantum Electron. **28**, 2423 (1992), and references therein.
[9] D. S. Kim, J. Shah, J. E. Cunningham, T. C. Damen, S. Schmitt-Rink, and W. Schäfer, Phys. Rev. Lett. **68**, 2838 (1992).
[10] D. S. Kim, J. Shah, T. C. Damen, W. Schäfer, F. Jahnke, S. Schmitt-Rink, and K. Köhler, Phys. Rev. Lett. **69**, 2725 (1992).
[11] A. Lohner, K. Rick, P. Leisching, A. Leitenstorfer, T. Elsaesser, T. Kuhn, F. Rossi, and W. Stolz, Phys. Rev. Lett. **71**, 77 (1993).
[12] M. D. Webb, S. T. Cundiff, and D. G. Steel, Phys. Rev. Lett. **66**, 934 (1991).
[13] K. Leo, T. C. Damen, J. Shah, E. O. Göbel, and K. Köhler, Appl. Phys. Lett. **57**, 19 (1990).
[14] K. Leo, T. C. Damen, J. Shah, and K. Köhler, Phys. Rev. B **42**, 11 359 (1990).
[15] K. Leo, E. O. Göbel, T. C. Damen, J. Shah, S. Schmitt-Rink, W. Schäfer, J. F. Müller, K. Köhler, and P. Ganser, Phys. Rev. B **44**, 5726 (1991).
[16] E. O. Göbel, K. Leo, T. C. Damen, J. Shah, S. Schmitt-Rink, W. Schäfer, J. F. Müller, and K. Köhler, Phys. Rev. Lett. **64**, 1801 (1990).
[17] M. Koch, J. Feldmann, G. von Plessen, E. O. Göbel, P. Thomas, and K. Köhler, Phys. Rev. Lett. **69**, 3631 (1992).
[18] A. E. Paul, W. Sha, S. Patkar, and A. L. Smirl, Phys. Rev. B **51**, 4242 (1995).
[19] A. L. Smirl, X. Chen, and O. Buccafusca, Opt. Lett. **23**, 1120 (1998).
[20] A. L. Smirl, X. Chen, and O. Buccafusca, IEEE J. Quantum Electron. **35**, 523 (1999).

[21] V. G. Lyssenko, J. Erland, I. Balslev, K.-H. Pantke, B. S. Razbirin, and J. M. Hvam, Phys. Rev. B **48**, 5720 (1993).
[22] S. Schmitt-Rink, D. Bennhardt, V. Heuckeroth, P. Thomas, P. Haring, G. Maidorn, H. Bakker, K. Leo, D. S. Kim, J. Shah, and K. Köhler, Phys. Rev. B **46**, 10 460 (1992).
[23] S. Patkar, A. E. Paul, W. Sha, J. A. Bolger, and A. L. Smirl, Phys. Rev. B **51**, 10 789 (1995).
[24] A. E. Paul, J. A. Bolger, and A. L. Smirl, J. Opt. Soc. Am. B **13**, 1016 (1996).
[25] J. A. Bolger, A. E. Paul, and A. L. Smirl, Phys. Rev. B **54**, 11 666 (1996).
[26] A. L. Smirl, W. J. Walecki, X. Chen, and O. Buccafusca, Phys. Status Solidi B **204**, 16 (1997).
[27] O. Buccafusca, X. Chen, W. J. Walecki, and A. L. Smirl, J. Opt. Soc. Am. B **15**, 1218 (1998).
[28] S. Weiss, M.-A. Mycek, J.-Y. Bigot, S. Schmitt-Rink, and D. S. Chemla, Phys. Rev. Lett. **69**, 2685 (1992).
[29] M. Wegener, D. S. Chemla, S. Schmitt-Rink, and W. Schäfer, Phys. Rev. A **42**, 5675 (1990).
[30] S. Schmitt-Rink, S. Mukamel, K. Leo, J. Shah, and D. S. Chemla, Phys. Rev. A **44**, 2124 (1991).
[31] W. Schäfer, F. Jahnke, and S. Schmitt-Rink, Phys. Rev. B **47**, 1217 (1993).
[32] H. Wang, K. Ferrio, D. G. Steel, Y. Z. Hu, R. Binder, and S. W. Koch, Phys. Rev. Lett. **71**, 1261 (1993).
[33] Y. Z. Hu, R. Binder, S. W. Koch, S. T. Cundiff, H. Wang, and D. G. Steel, Phys. Rev. B **49**, 14 382 (1994).
[34] T. Rappen, U. G. Peter, M. Wegener, and W. Schäfer, Phys. Rev. B **49**, 10 774 (1994).
[35] D. G. Steel, H. Wang, M. Jiang, K. Farrio, and S. T. Cundiff, in *Coherent Optical Interactions in Semiconductors*, edited by R. T. Phillips (Plenum, New York, 1994), pp. 157–179.
[36] B. F. Feuerbacher, J. Kuhl, and K. Ploog, Phys. Rev. B **43**, 2439 (1991).
[37] S. Bar-Ad and I. Bar-Joseph, Phys. Rev. Lett. **68**, 349 (1992).
[38] H. H. Yaffe, Y. Prior, J. P. Harbison, and L. T. Florez, J. Opt. Soc. Am. B **10**, 578 (1993).
[39] H. Wang, J. Shah, T. C. Damen, and L. N. Pfeiffer, Solid State Commun. **91**, 869 (1994).
[40] T. Saiki, M. Kuwata-Gonokami, T. Matsusue, and H. Sakaki, Phys. Rev. B **49**, 7817 (1994).
[41] E. J. Mayer, G. O. Smith, V. Heuckeroth, J. Kuhl, K. Bott, A. Schulze, T. Meier, D. Bennhardt, S. W. Koch, P. Thomas, R. Hey, and K. Ploog, Phys. Rev. B **50**, 14 730 (1994).
[42] K.-H. Pantke, D. Oberhauser, V. G. Lyssenko, J. M. Hvam, and G. Weimann, Phys. Rev. B **47**, 2413 (1993).
[43] K. Bott, O. Heller, D. Bennhardt, S. T. Cundiff, P. Thomas, E. J. Mayer, G. O. Smith, R. Eccleston, J. Kuhl, and K. Ploog, Phys. Rev. B **48**, 17 418 (1993).
[44] W. Schäfer and J. Treusch, Z. Phys. B **63**, 407 (1986).
[45] R. Zimmermann, *Many-Particle Theory of Highly Excited Semiconductors* (Teubner, Leipzig, 1988).
[46] H. Haug and S. W. Koch, *Quantum Theory of the Optical and Electronic Properties of Semiconductors* (World Scientific, Singapore, 1993).
[47] R. Binder and S. W. Koch, Prog. Quantum Electron. **19**, 307 (1995).
[48] H. Haug and A. P. Jauho, *Quantum Kinetics in Transport and Optics of Semiconductors* (Springer, Berlin, 1996).
[49] R. Zimmermann, K. Kilimann, W. D. Kraeft, D. Kremp, and G. Röpke, Phys. Status Solidi B **90**, 175 (1978).
[50] W. Schäfer, K. H. Schuldt, and R. Binder, Phys. Status Solidi B **150**, 407 (1988).
[51] C. Sieh, T. Meier, F. Jahnke, A. Knorr, S. W. Koch, P. Brick, M. Hübner, C. Ell, J. Prineas, G. Kitrova, and H. M. Gibbs, Phys. Rev. Lett. **82**, 3112 (1999).
[52] V. M. Axt and A. Stahl, Z. Phys. B **93**, 195 (1994); **93**, 205 (1994).
[53] M. Z. Maialle and L. J. Sham, Phys. Rev. Lett. **73**, 3310 (1994).
[54] P. Kner, S. Bar-Ad, M. V. Marquezini, D. S. Chemla, and W. Schäfer, Phys. Rev. Lett. **78**, 1319 (1997).
[55] W. J. Walecki, D. N. Fittinghoff, A. L. Smirl, and R. Trebino, Opt. Lett. **22**, 81 (1997).
[56] K. W. DeLong, R. Trebino, J. Hunter, and W. E. White, J. Opt. Soc. Am. B **11**, 2206 (1994), and references therein.
[57] L. Lepetit, G. Chériaux, and M. Joffre, J. Opt. Soc. Am. B **12**, 2467 (1995).
[58] D. N. Fittinghoff, J. L. Bowie, J. N. Sweetser, R. T. Jennings, M. A. Krumbügel, K. W. DeLong, R. Trebino, and I. A. Walmsey, Opt. Lett. **21**, 884 (1996).
[59] H. P. Wagner, W. Langbein, and J. M. Hvam, Phys. Rev. B **59**, 4584 (1999).
[60] Th. Östreich, K. Schönhammer, and L. J. Sham, Phys. Rev. Lett. **74**, 4698 (1995).
[61] K. B. Ferrio and D. G. Steel, Phys. Rev. Lett. **80**, 786 (1998).
[62] M. Phillips and H. Wang, Solid State Commun. **111**, 317 (1999).